



Published in final edited form as:

*Mol Imaging Biol.* 2011 April ; 13(2): 215–221. doi:10.1007/s11307-010-0353-6.

## Biodistribution and Clearance of Small Molecule Hapten Chelates for Pretargeted Radioimmunotherapy

Kelly Davis Orcutt<sup>1</sup>, Khaled A. Nasr<sup>4</sup>, David G. Whitehead<sup>4</sup>, John V. Frangioni<sup>4,5</sup>, and K. Dane Wittrup<sup>1,2,3</sup>

<sup>1</sup>Department of Chemical Engineering, Massachusetts Institute of Technology, 400 Main Street E19-551, Cambridge, MA 02139, USA

<sup>2</sup>Department of Biological Engineering, Massachusetts Institute of Technology, Cambridge, MA 02139, USA

<sup>3</sup>Koch Institute for Integrative Cancer Research, Massachusetts Institute of Technology, Cambridge, MA 02139, USA

<sup>4</sup>Division of Hematology/Oncology, Beth Israel Deaconess Medical Center, Boston, MA 02215, USA

<sup>5</sup>Department of Medicine, Beth Israel Deaconess Medical Center, Boston, MA 02215, USA

### Abstract

**Purpose**—The favorable pharmacokinetics and clinical safety profile of metal-chelated 1,4,7,10-tetraazacyclododecane-1,4,7,10-tetraacetic acid (DOTA) suggests that it might be an ideal hapten for pretargeted radioimmunotherapy. In an effort to minimize hapten retention in normal tissues and determine the effect of various chemical adducts on *in vivo* properties, a series of DOTA-based derivatives were evaluated.

**Procedures**—Biodistribution and whole-body clearance were evaluated for <sup>177</sup>Lu-labeled DOTA, DOTA-biotin, a di-DOTA peptide, and DOTA-aminobenzene in normal CD1 mice. Kidney, liver, and bone marrow doses were estimated using standard Medical Internal Radiation Dose methodology.

**Results**—All haptens demonstrated similar low tissue and whole-body retention, with 2–4% of the injected dose remaining in mice 4 h postinjection. The kidney is predicted to be dose limiting for all <sup>177</sup>Lu-labeled haptens tested with an estimated kidney dose of approximately 0.1 mGy/MBq.

**Conclusions**—We present here a group of DOTA-based haptens that exhibit rapid clearance and exceptionally low whole-body retention 4 h postinjection. Aminobenzene, tyrosine-lysine, and biotin groups have minimal effects on the blood clearance and biodistribution of <sup>177</sup>Lu-DOTA.

### Keywords

Pretargeted radioimmunotherapy; DOTA; Biodistribution; Clearance; Radiation dosimetry

## Introduction

Pretargeted radioimmunotherapy (PRIT) strategies for cancer have been investigated for the past 20 years [1–3]. In PRIT, a nonradioactive bifunctional antibody with specificity for both a tumor antigen and a small molecule hapten is administered and allowed to localize to the tumor(s). After sufficient blood clearance of the antibody (or a clearing step to reduce subsequent hapten binding to residual antibody in the blood), a radiolabeled small molecule is administered and captured by the pretargeted antibody (Fig. 1). This strategy combines the high binding specificity of antibodies with the fast blood clearance of small molecules, resulting in higher tumor-to-blood ratios than directly radiolabeled antibody targeting [4–7].

The first PRIT systems used streptavidin antibody fusions and biotinylated haptens. However, binding of endogenous biotin to pretargeted streptavidin reduces efficacy [8]. In addition, streptavidin is immunogenic and exhibits high renal uptake [9] resulting in high radiation dose to the kidneys. Thus, recent efforts in PRIT have moved away from streptavidin systems and have focused on the development of bispecific antibodies with affinity for metal chelates or peptide moieties [10, 11].

One very important step in the development of PRIT approaches is the selection of the hapten. The hapten must be nontoxic, not endogenous, not metabolized, and must clear rapidly from the blood with minimal normal tissue retention. While many small peptides and metal chelates exhibit fast renal clearance, most exhibit significant whole-body retention [10, 12–19]. This background retention is typically 10–30% injected dose (ID) at 2 to 4 h postinjection (summarized in Table 1). Significant whole-body retention results in background activity limiting signal-to-background ratios for imaging and contributing to nonspecific radiation limiting the maximum tolerated dose for therapy applications. Identifying small molecules with low whole-body retention is thus necessary for improving both imaging and therapy with radioisotopes.

The present study focuses on the use of 1,4,7,10-tetraazacyclododecane-1,4,7,10-tetraacetic acid (DOTA) as a possible hapten for PRIT because of its ability to chelate a wide variety of isotopes useful for imaging and therapy [20] and its history of safe use in humans as an MRI contrast agent (chelated to Gd) [21, 22]. DOTA-Gd is not endogenous, not metabolized, and exhibits rapid blood clearance.

Recently, we developed a high-affinity antibody-binding fragment to DOTA metal chelates (Orcutt et al., manuscript in review). The engineered single chain variable domain (scFv) binds to yttrium and lutetium DOTA-chelates with 100 pM affinity and DOTA-aminobenzene-chelates with 10 pM affinity. We have engineered this scFv into a novel IgG-like bispecific antibody format that retains parental affinities and exhibits IgG-like *in vivo* blood pharmacokinetics and tumor targeting [23].

In the present study, we are interested in investigating the *in vivo* biodistribution and clearance of various small molecule haptens to determine the effects of various adducts on the *in vivo* properties of DOTA. Currently, it is not known *a priori* how the addition of chemical groups will affect the *in vivo* properties of small molecules. Even small chemical modifications can drastically change retention and background [24]. Our efforts are 2-fold: (1) to increase the knowledge base of *in vivo* behavior of various DOTA-based compounds in an effort to develop a more comprehensive understanding to aid in the future development of molecular imaging and therapeutic agents with low background and (2) to determine what form(s) of the DOTA chelate will result in the fastest blood clearance and lowest whole-body and kidney retention for PRIT applications. This quantitative analysis is crucial in moving toward an end goal of minimizing radioisotope retention in normal tissues.

## Materials and Methods

### Reagents

DOTA, *S*-2-(*R*-aminobenzyl)-1,4,7,10-tetraazacyclododecane tetra-acetic acid (DOTA-Bn), DOTA-biotin-sarcosine (DOTA-biotin), and 1,4,7,10-tetraazacyclododecane-1,4,7,10-tetraacetic acid mono (*N*-hydroxysuccinimide ester) (DOTA-NHS) were purchased from Macrocyclics (Dallas, TX, USA). Tyrosine-lysine peptide was purchased from Anaspec (San Jose, CA, USA). All other chemicals were purchased from Sigma-Aldrich (St. Louis, MO, USA) or Thermo Fisher Scientific (Waltham, MA, USA).

### DOTATyrLysDOTA Synthesis

DOTATyrLysDOTA was synthesized by reacting a 10-fold molar excess of DOTA-NHS with tyrosine-lysine peptide in dimethyl sulfoxide in the presence of a 20-fold molar excess of triethylamine. The reaction was vortexed for 3 h at room temperature. To confirm completion of the reaction, the reaction mixture was analyzed by reverse-phase high-performance liquid chromatography (HPLC) as described previously [25] using a Waters 4.6 × 150 mm Symmetry C18 column and a linear gradient from 0% to 40% *B* in 25 min at 1 mL/min with *A*=water+0.1% formic acid and *B*=acetonitrile+0.1% formic acid. DOTATyrLysDOTA eluted at a retention time ( $R_t$ )=9.6 min as detected by evaporative light scatter detector (ELSD), with the mass confirmed by electrospray time-of-flight mass spectrometry, calculated  $m/z$  1,082.53 [M+H]<sup>+</sup>, found 1,083.19 [M+H]<sup>+</sup>. Preparative purification was performed on an HPLC system using a 19×150-mm Symmetry C18 column with a linear gradient of 0% *B* to 40% *B* in 35 min with *A*=water+0.1% formic acid and *B*=acetonitrile+0.1% formic acid. DOTATyrLysDOTA eluted at  $R_t$ =5.6 min using ELSD detection. Fractions containing product were pooled and lyophilized. Purity was confirmed by analytical HPLC.

### Radiolabeling

The HPLC/mass spectrometry platform used for purification of radioactive small molecules and peptides has been described in detail [25, 26]. Compounds were dissolved at 0.5 mM in ammonium acetate pH 5.6; 1 to 2 mCi <sup>177</sup>LuCl<sub>3</sub> (PerkinElmer, Waltham, MA, USA) were added to the metal chelate and incubated for 1 to 2 h at 85–95°C. The radiolabeled compounds were purified by RP-HPLC with gamma detection on a 4.6×75-mm Symmetry C18 column using a linear gradient from 0% to 90% *B* over 15 min, at a flow rate of 1 mL/min, where *A*=water and *B*=acetonitrile. The compounds were then dried under vacuum, resuspended in saline, and filter-sterilized.

### Animal Models

All animal handling was performed in accordance with Beth Israel Deaconess Medical Center Animal Research Committee guidelines. CD1 male mice were purchased from Taconic Farms (Germantown, NY, USA). For biodistribution and clearance testing, 50–150 μCi <sup>177</sup>Lu-labeled hapten was injected intravenously into the mice. Blood was collected from the tail vein using microcapillary tubes and counted on a model 1470 Wallac Wizard (Perkin Elmer, Wellesley, MA, USA) ten-detector gamma counter. Mice were euthanized by intraperitoneal injection of pentobarbital followed by cervical dislocation, a method consistent with the recommendations of the Panel on Euthanasia of the American Veterinary Medical Association. Whole-body retention of radioactivity was measured in a dose calibrator after removing the bladder en masse. Organs were resected, washed in phosphate buffered saline thrice, weighed, and counted as described above.

## Statistics

Differences between means of organ/tissue uptake and blood clearance parameters were assessed using a two-tailed Student's *T* test with *P* values <0.05 considered significant. Blood clearance parameters were calculated by a least squares biexponential fit of the percent injected dose per gram versus time data.

## Dosimetry

Radiation doses absorbed by normal tissues were calculated according to the Medical Internal Radiation Dose (MIRD) scheme. Percent injected activity in kidneys, liver, and whole body were calculated from activity measurements. Isotope decay-adjusted activity was integrated over time, with a conservative assumption that the 24-h organ %ID remained constant thereafter for the liver, kidneys, and whole body. *S* values (the absorbed dose per unit cumulated activity) for <sup>90</sup>Y, <sup>131</sup>I, and <sup>177</sup>Lu were used to calculate dosimetry estimates in an adult male reference [27]. The blood activity data were fit to a biexponential function and used to determine the red marrow dose as described [28]. The activity in the whole body was used to estimate the total body cumulative activity used for cross-dose calculations.

## Estimation of Whole-Body Retention for Published Haptens

For each molecule, a lower limit for the whole-body %ID was calculated by summing the %ID of each measured organ from the published average %ID/g multiplied by the organ weight. Where organ weight information was unavailable, we assumed a 25-g mouse with the following distribution of organ weight percent: blood 8%, skin 11.2%, adipose 20%, muscle 40%, bone 7.5%, heart 0.43%, lung 0.56%, spleen 0.42%, liver 6.4%, kidneys 1.5%, stomach 0.9%, large intestine 1.78%, small intestine 2.75%, pancreas 0.3%, and brain 1.38%.

## Results

The *in vivo* blood clearance and organ biodistribution of four <sup>177</sup>Lu-labeled DOTA haptens (Fig. 2) were studied to determine how various small molecule appendages (amino-benzene, biotin, and a small peptide) affect *in vivo* tissue retention and clearance of DOTA. Serial blood samples were taken to determine blood clearance of the haptens (Fig. 3). DOTA cleared faster from the blood than the other haptens tested; blood activity was not distinguishable from background after 2 h. The blood activity for all other haptens tested was not distinguishable above background after 3 h. Blood activity data were fit to biexponential functions and the blood clearance parameters reported in Table 2. The  $\alpha$  phase clearance for <sup>177</sup>Lu-DOTA was significantly (*P*<0.05) faster than that for <sup>177</sup>Lu-DOTA-benzene while the  $\beta$  phase clearance for <sup>177</sup>Lu-DOTA was significantly (*P*<0.05) faster than that for <sup>177</sup>Lu-DOTA-biotin. Mice were euthanized 4 and 24 h postinjection to determine organ biodistribution (Fig. 4). Tissue uptake was relatively low for all haptens. The %ID remaining in the whole animal was approximately 2–4% at 4 h and 1–3% at 24 h for the haptens, significantly lower than many other radiolabeled small molecules reported in the literature (summarized in Table 1). There were few statistically significant differences in the organ biodistribution of the four haptens (Fig. 4).

From the organ biodistribution data, the radiation dose to the liver, kidney, and bone marrow was estimated for a 70-kg man for three radioisotopes, <sup>90</sup>Y, <sup>131</sup>I, and <sup>177</sup>Lu (Table 3). The self-dose and the total dose (self-dose plus cross-dose) are provided, where the whole-body activity was used to determine the cross-dose. From the dose estimates, it is apparent that the cross-dose from the whole-body activity significantly impacts the dose to the red marrow, increasing the dose by 10- to 70-fold.

The dose-limiting toxicities ( $TD_{5/5}$ ) for the liver, kidney, and red marrow estimated from external beam radiation are 30, 23, and 1.5 Gy, respectively [29]. From the radiation dose estimates for the haptens, the dose-limiting organ is predicted to be the kidney for all  $^{177}\text{Lu}$ -labeled haptens tested with an estimated kidney dose of approximately 0.1 mGy/MBq and liver and red marrow doses of approximately 0.01–0.02 mGy/MBq and  $2$  to  $3 \times 10^{-3}$  mGy/MBq, respectively. However, for  $^{90}\text{Y}$  and  $^{131}\text{I}$  isotopes, the dose-limiting organ could be either the kidneys or the red marrow, with less than a 2-fold difference predicted between the two organs for the estimated dose normalized to the respective organ  $TD_{5/5}$ . The estimated liver, kidney, and red marrow doses for  $^{90}\text{Y}$ -labeled haptens are 0.04–0.05, 0.2–0.3, and 0.01 mGy/MBq, respectively, and 0.02–0.04, 0.1–0.2, and 0.01–0.02 mGy/MBq, respectively, for  $^{131}\text{I}$ -labeled haptens.

## Discussion

In this study, we present a group of small molecule DOTA-based compounds that exhibit rapid blood clearance and result in exceptionally low whole-body retention within 4 h postinjection. While many small molecules exhibit fast blood clearance, they generally exhibit significant retention in normal tissues (Table 1). This background whole-body retention is typically 10–30% at 2–4 h and results in background radiation that limits signal-to-background ratios for imaging and nonspecific radiation that contributes to maximum tolerated dose for therapy applications. Identifying small molecules that exhibit whole-body retention less than 5% in only a few hours is thus necessary for improving both imaging and therapy using radionuclides. The DOTA molecules we present here should thus prove exceptionally useful for pretargeted applications with bispecific antibodies. The development of small molecules with even lower whole-body retention would further improve tumor-to-off-target ratios.

Other small molecules have been developed for pretargeted applications including DOTA-biotin as well as small peptide haptens [10, 30]. The streptavidin/ $^{90}\text{Y}$ -DOTA-biotin PRIT system has been tested clinically, and radiation doses have been estimated from whole-body scintigraphy at approximately  $3.5 \pm 1.0$  and  $0.04 \pm 0.01$  mGy/MBq for the kidneys and red marrow, respectively [31]. The predicted dose estimates for the  $^{90}\text{Y}$ -DOTA-biotin hapten presented here are 0.18 and 0.011 mGy/MBq for the kidney and red marrow, respectively. Thus, the kidney dose for the hapten is predicted to be about 20-fold lower than that measured in the clinical PRIT study. This is expected as streptavidin localizes to the kidneys where it remains accessible to binding by DOTA-biotin [9]. In a mouse lymphoma xenograft study, pretargeted DOTA-biotin exhibited about 5- to 10-fold higher kidney uptake than DOTA-biotin alone [32]. In addition to high streptavidin uptake in the kidneys, streptavidin pretargeted systems also suffer from endogenous biotin binding to streptavidin [8]. Thus, recent efforts have moved toward approaches using bispecific antibodies with peptide haptens. Sharkey et al. have developed an approach using peptide-based haptens and an antibody that recognizes the peptide epitope [10]. While some of these peptide-based haptens exhibit fast clearance and low tissue uptake, others exhibit significantly slower whole-body clearance [10].

We are interested in developing a nonpeptide approach using DOTA-based haptens. It was expected that an approach without using peptides would reduce kidney uptake, as it is known that peptides exhibit tubular reabsorption and resulting kidney retention [33]. However, the data presented here show no significant difference in kidney retention between DOTA and the DOTATyrLys-DOTA peptide. From MIRD radiation dose estimates, similar red marrow doses are predicted for DOTA and the peptide. Nevertheless, DOTA presents some potential advantages as a hapten for PRIT. DOTA is commercially available in large quantities, and thus, no further synthesis before radiolabeling is required. In addition, Gd-

DOTA, injected in millimolar quantities for MRI imaging, has an established safety profile in humans [22].

In addition to the DOTATyrLysDOTA peptide, we analyzed *in vivo* clearance and biodistribution of DOTA-biotin and DOTA-benzene. DOTA-biotin has been used extensively as a hapten for PRIT, yet there is no literature to our knowledge of the effect of biotin on biodistribution and clearance.  $^{177}\text{Lu}$ -DOTA-benzene is of interest to us, as it exhibits 10-fold higher binding affinity than  $^{177}\text{Lu}$ -DOTA to a recently engineered high-affinity DOTA-binding antibody fragment (Orcutt et al., manuscript in review). Here, we show that both the biotin and aminobenzene adducts have minimal effects on biodistribution and blood clearance of  $^{177}\text{Lu}$ -DOTA (Table 2, Figure 4).

From dosimetry estimates, it is predicted that the dose-limiting toxicity for all of the hapten molecules radiolabeled with Lu-177 is the kidney. However, for Y-90 and I-131 isotopes with longer path lengths, whole-body retention of the hapten contributes significantly to the red marrow dose, resulting in similar estimated doses to  $\text{TD}_{5/5}$  ratios for the kidney and the red marrow. These estimates are for the hapten molecule alone. In PRIT, residual bispecific antibody in the blood and nontumor tissue will bind to the hapten and may significantly alter clearance and biodistribution. Clinical PRIT studies with I-131 without a clearing or blocking agent report hematological toxicity as dose limiting [34].

Directly radiolabeled antibodies in radioimmunotherapy trials exhibit dose-limiting hematological toxicity, with estimated doses of  $2.7 \pm 0.9$  mGy/MBq to the marrow and  $2.4 \pm 0.6$  mGy/MBq dose to the kidneys when using Y-90 [35]. This suggests that if residual bispecific antibody is sufficiently low, PRIT will result in significantly higher tumor-to-marrow and tumor-to-kidney ratios. In addition, the results presented here suggest that Lu-177 may result in lower off-target doses and may be preferred over Y-90 and I-131 in PRIT applications; this has also been suggested for radioimmunotherapy based on a xenograft study [36].

In cases where the kidney proves to be the dose-limiting organ, kidney uptake and radiation dose may be reduced by using diuretics, catheterization, and/or renal protective agents [37].

## Conclusion

In an effort to minimize hapten retention in normal tissue for PRIT applications, a series of DOTA-based derivatives were evaluated for blood clearance and organ biodistribution *in vivo* in CD1 mice. The blood clearance was rapid for all compounds, and there were few statistically significant differences between the average organ/tissue activities at 4 and 24 h post injection (p.i.) and fit blood clearance parameters. The carcass retention values were approximately 2–4% at 4 h and 1–3% at 24 h p.i. We thus conclude that all DOTA compounds tested behave similarly *in vivo* and exhibit low whole-body retention.

## Acknowledgments

The authors acknowledge Elaine P. Lunsford and Gaurav Gulati for technical assistance and Hak Soo Choi for helpful discussions. This work was supported by the Lewis Family Fund (JVF), National Institutes of Health grant R01-CA-101830 (KDW), and a National Science Foundation Graduate Research Fellowship (KDO).

## References

1. Boerman OC, van Schaijk FG, Oyen WJ, Corstens FH. Pretargeted radioimmunotherapy of cancer: progress step by step. *J Nucl Med.* 2003; 44:400–411. [PubMed: 12621007]



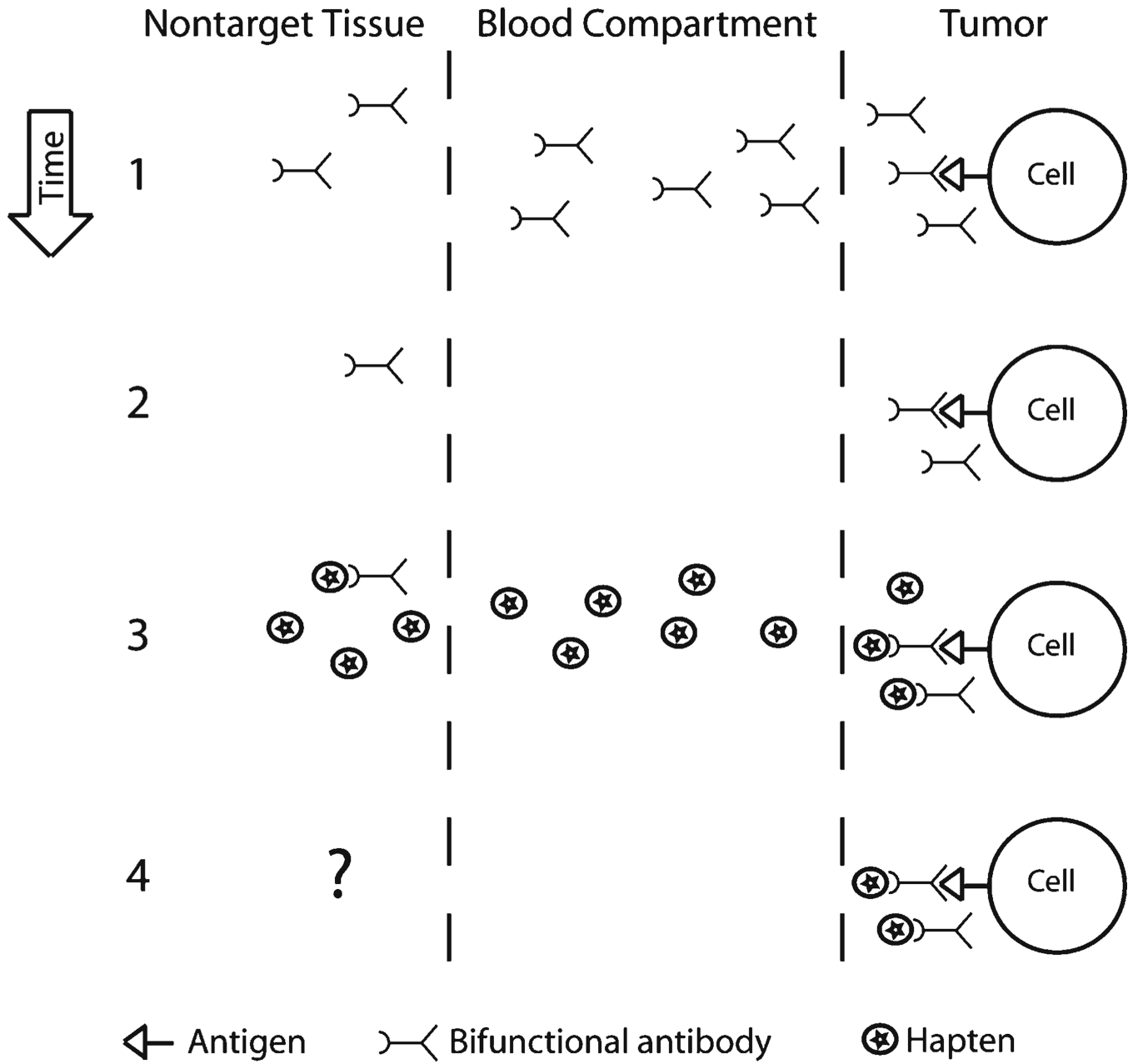
2. Gruaz-Guyon A, Raguin O, Barbet J. Recent advances in pretargeted radioimmunotherapy. *Curr Med Chem*. 2005; 12:319–338. [PubMed: 15723622]
3. Goodwin DA, Meares CF, McCall MJ, McTigue M, Chaovapong W. Pre-targeted immunoscintigraphy of murine tumors with indium-111-labeled bifunctional haptens. *J Nucl Med*. 1988; 29:226–234. [PubMed: 3346734]
4. Axworthy DB, Reno JM, Hyilarides MD, et al. Cure of human carcinoma xenografts by a single dose of pretargeted yttrium-90 with negligible toxicity. *Proc Natl Acad Sci USA*. 2000; 97:1802–1807. [PubMed: 10677537]
5. Subbiah K, Hamlin DK, Pagel JM, et al. Comparison of immunoscintigraphy, efficacy, and toxicity of conventional and pretargeted radioimmunotherapy in CD20-expressing human lymphoma xenografts. *J Nucl Med*. 2003; 44:437–445. [PubMed: 12621012]
6. Pagel JM, Orgun N, Hamlin DK, et al. A comparative analysis of conventional and pretargeted radioimmunotherapy of B-cell lymphomas by targeting CD20, CD22, and HLA-DR singly and in combinations. *Blood*. 2009; 113:4903–4913. [PubMed: 19124831]
7. Sharkey RM, Karacay H, Johnson CR, et al. Pretargeted versus directly targeted radioimmunotherapy combined with anti-CD20 antibody consolidation therapy of non-Hodgkin lymphoma. *J Nucl Med*. 2009; 50:444–453. [PubMed: 19223402]
8. Hamblett KJ, Kegley BB, Hamlin DK, et al. A streptavidin–biotin binding system that minimizes blocking by endogenous biotin. *Bioconjug Chem*. 2002; 13:588–598. [PubMed: 12009950]
9. Forster GJ, Santos EB, Smith-Jones PM, Zanzonico P, Larson SM. Pretargeted radioimmunotherapy with a single-chain antibody/streptavidin construct and radiolabeled DOTA-biotin: strategies for reduction of the renal dose. *J Nucl Med*. 2006; 47:140–149. [PubMed: 16391198]
10. Sharkey RM, McBride WJ, Karacay H, et al. A universal pretargeting system for cancer detection and therapy using bispecific antibody. *Cancer Res*. 2003; 63:354–363. [PubMed: 12543788]
11. Gautherot E, Rouvier E, Daniel L, et al. Pretargeted radio-immunotherapy of human colorectal xenografts with bispecific antibody and 131I-labeled bivalent hapten. *J Nucl Med*. 2000; 41:480–487. [PubMed: 10716323]
12. Chen X, Park R, Tohme M, et al. MicroPET and autoradiographic imaging of breast cancer alpha v-integrin expression using 18F- and 64Cu-labeled RGD peptide. *Bioconjug Chem*. 2004; 15:41–49. [PubMed: 14733582]
13. Chen X, Sievers E, Hou Y, et al. Integrin alpha v beta 3-targeted imaging of lung cancer. *Neoplasia*. 2005; 7:271–279. [PubMed: 15799827]
14. Garrison JC, Rold TL, Sieckman GL, et al. *In vivo* evaluation and small-animal PET/CT of a prostate cancer mouse model using 64Cu bombesin analogs: side-by-side comparison of the CB-TE2A and DOTA chelation systems. *J Nucl Med*. 2007; 48:1327–1337. [PubMed: 17631556]
15. Zhang H, Schuhmacher J, Waser B, et al. DOTA-PESIN, a DOTA-conjugated bombesin derivative designed for the imaging and targeted radionuclide treatment of bombesin receptor-positive tumours. *Eur J Nucl Med Mol Imaging*. 2007; 34:1198–1208. [PubMed: 17262215]
16. Schmitt A, Bernhardt P, Nilsson O, et al. Differences in biodistribution between 99mTc-depreotide, 111In-DTPA-octreotide, and 177Lu-DOTA-Tyr3-octreotate in a small cell lung cancer animal model. *Cancer Biother Radiopharm*. 2005; 20:231–236. [PubMed: 15869461]
17. Wild D, Behe M, Wicki A, et al. [Lys40(Ahx-DTPA-111In)NH2] exendin-4, a very promising ligand for glucagon-like peptide-1 (GLP-1) receptor targeting. *J Nucl Med*. 2006; 47:2025–2033. [PubMed: 17138746]
18. Haubner R, Wester HJ, Burkhart F, et al. Glycosylated RGD-containing peptides: tracer for tumor targeting and angiogenesis imaging with improved biokinetics. *J Nucl Med*. 2001; 42:326–336. [PubMed: 11216533]
19. Ferreira CL, Lamsa E, Woods M, et al. Evaluation of bifunctional chelates for the development of gallium-based radiopharmaceuticals. *Bioconjug Chem*. 2010; 21:531–536. [PubMed: 20175523]
20. Cutler CS, Smith CJ, Ehrhardt GJ, et al. Current and potential therapeutic uses of lanthanide radioisotopes. *Cancer Biother Radiopharm*. 2000; 15:531–545. [PubMed: 11190486]
21. Le Mignon MM, Chambon C, Warrington S, Davies R, Bonnemain B. Gd-DOTA. Pharmacokinetics and tolerability after intravenous injection into healthy volunteers. *Invest Radiol*. 1990; 25:933–937. [PubMed: 2394577]

22. Bourrinet P, Martel E, El Amrani AI, et al. Cardiovascular safety of gadoterate meglumine (Gd-DOTA). *Invest Radiol.* 2007; 42:63–77. [PubMed: 17220724]
23. Orcutt KD, Ackerman ME, Cieslewicz M, et al. A modular IgG-scFv bispecific antibody topology. *Protein Eng Des Sel.* 2010; 23:221–228. [PubMed: 20019028]
24. Banerjee SR, Foss CA, Castanares M, et al. Synthesis and evaluation of technetium-99m- and rhenium-labeled inhibitors of the prostate-specific membrane antigen (PSMA). *J Med Chem.* 2008; 51:4504–4517. [PubMed: 18637669]
25. Humblet V, Misra P, Frangioni JV. An HPLC/mass spectrometry platform for the development of multimodality contrast agents and targeted therapeutics: prostate-specific membrane antigen small molecule derivatives. *Contrast Media Mol Imaging.* 2006; 1:196–211. [PubMed: 17193697]
26. Misra P, Humblet V, Pannier N, Maison W, Frangioni JV. Production of multimeric prostate-specific membrane antigen small-molecule radiotracers using a solid-phase <sup>99m</sup>Tc preloading strategy. *J Nucl Med.* 2007; 48:1379–1389. [PubMed: 17631555]
27. Stabin MG, Siegel JA. Physical models and dose factors for use in internal dose assessment. *Health Phys.* 2003; 85:294–310. [PubMed: 12938720]
28. Wessels BW, Bolch WE, Bouchet LG, et al. Bone marrow dosimetry using blood-based models for radiolabeled antibody therapy: a multiinstitutional comparison. *J Nucl Med.* 2004; 45:1725–1733. [PubMed: 15471841]
29. Emami B, Lyman J, Brown A, et al. Tolerance of normal tissue to therapeutic irradiation. *Int J Radiat Oncol Biol Phys.* 1991; 21:109–122. [PubMed: 2032882]
30. Barbet J, Peltier P, Bardet S, et al. Radioimmunodetection of medullary thyroid carcinoma using indium-111 bivalent hapten and anti-CEA × anti-DTPA-indium bispecific antibody. *J Nucl Med.* 1998; 39:1172–1178. [PubMed: 9669389]
31. Knox SJ, Goris ML, Tempero M, et al. Phase II trial of yttrium-90-DOTA-biotin pretargeted by NR-LU-10 antibody/streptavidin in patients with metastatic colon cancer. *Clin Cancer Res.* 2000; 6:406–414. [PubMed: 10690517]
32. Lin Y, Pagel JM, Axworthy D, et al. A genetically engineered anti-CD45 single-chain antibody–streptavidin fusion protein for pretargeted radioimmunotherapy of hematologic malignancies. *Cancer Res.* 2006; 66:3884–3892. [PubMed: 16585217]
33. Behr TM, Goldenberg DM, Becker W. Reducing the renal uptake of radiolabeled antibody fragments and peptides for diagnosis and therapy: present status, future prospects and limitations. *Eur J Nucl Med.* 1998; 25:201–212. [PubMed: 9473271]
34. Kraeber-Bodere F, Rousseau C, Bodet-Milin C, et al. Targeting, toxicity, and efficacy of 2-step, pretargeted radioimmunotherapy using a chimeric bispecific antibody and <sup>131</sup>I-labeled bivalent hapten in a phase I optimization clinical trial. *J Nucl Med.* 2006; 47:247–255. [PubMed: 16455630]
35. Fisher DR, Shen S, Meredith RF. MIRD dose estimate report No. 20: radiation absorbed-dose estimates for <sup>111</sup>In- and <sup>90</sup>Y-ibritumomab tiuxetan. *J Nucl Med.* 2009; 50:644–652. [PubMed: 19289440]
36. Zacchetti A, Coliva A, Luison E, et al. (<sup>177</sup>)Lu- labeled MOv18 as compared to (<sup>131</sup>)I- or (<sup>90</sup>)Y-labeled MOv18 has the better therapeutic effect in eradication of alpha folate receptor-expressing tumor xenografts. *Nucl Med Biol.* 2009; 36:759–770. [PubMed: 19720288]
37. Jaggi JS, Seshan SV, McDevitt MR, et al. Mitigation of radiation nephropathy after internal alpha-particle irradiation of kidneys. *Int J Radiat Oncol Biol Phys.* 2006; 64:1503–1512. [PubMed: 16503385]

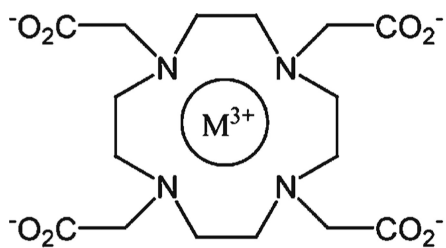
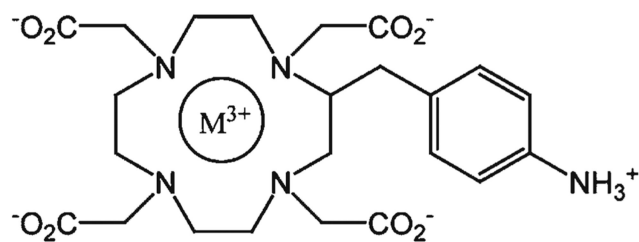
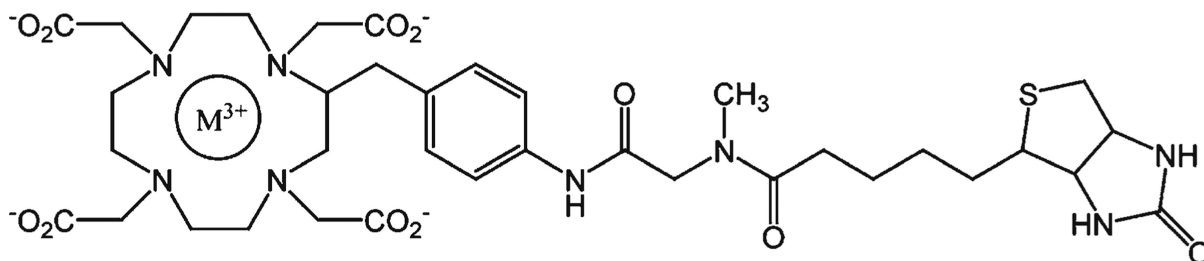
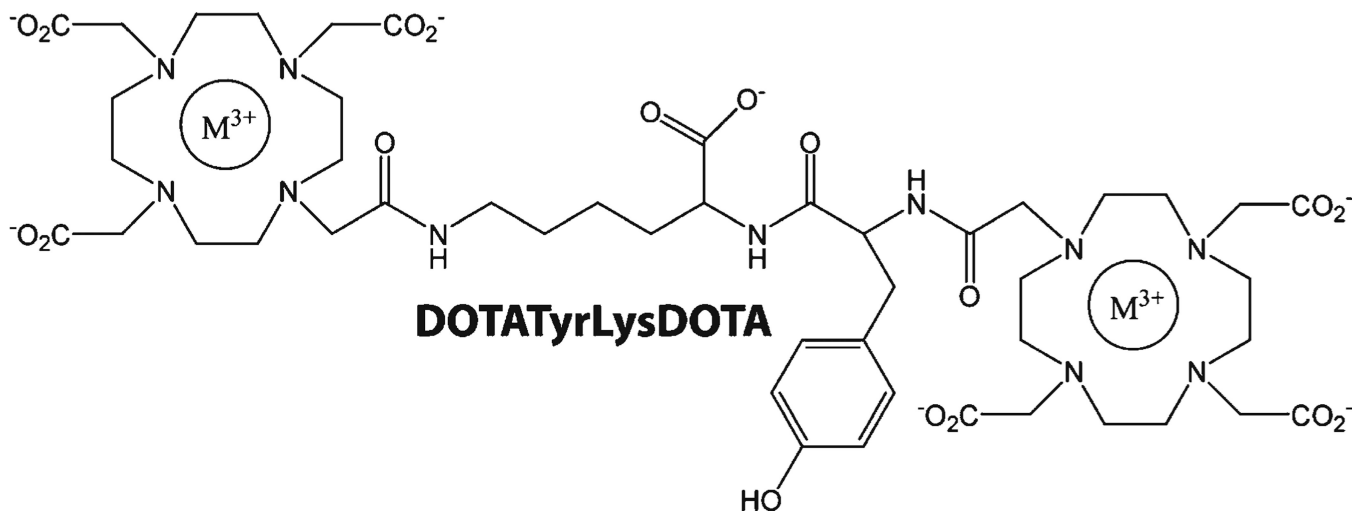


### Significance

We present here a quantitative *in vivo* analysis of four  $^{177}\text{Lu}$ -labeled DOTA-based small molecules in an effort to determine what form(s) of the DOTA chelate result in the fastest clearance and lowest tissue retention for pretargeted radioimmunotherapy applications and also to determine how various chemical moieties affect *in vivo* behavior of small molecules.



**Fig. 1.** Schematic of pretargeted radioimmunotherapy. A pictorial representation of PRIT where a bifunctional antibody is administered in step 1. In step 2, the antibody is cleared from the body over time and/or with the help of a synthetic clearing agent (clearing agent not depicted). In step 3, a radiolabeled hapten is administered. In step 4, the hapten is cleared from the body over time; in this study, we investigate tissue and whole-body retention of various haptens.

**DOTA****DOTA-Benzene****DOTA-Biotin****DOTATyrLysDOTA**

**Fig. 2.** Chemical structures of DOTA-based small molecule haptens. Chemical structures of DOTA-based haptens. M<sup>3+</sup> = trivalent cation metal = <sup>177</sup>Lu in all experiments presented here.

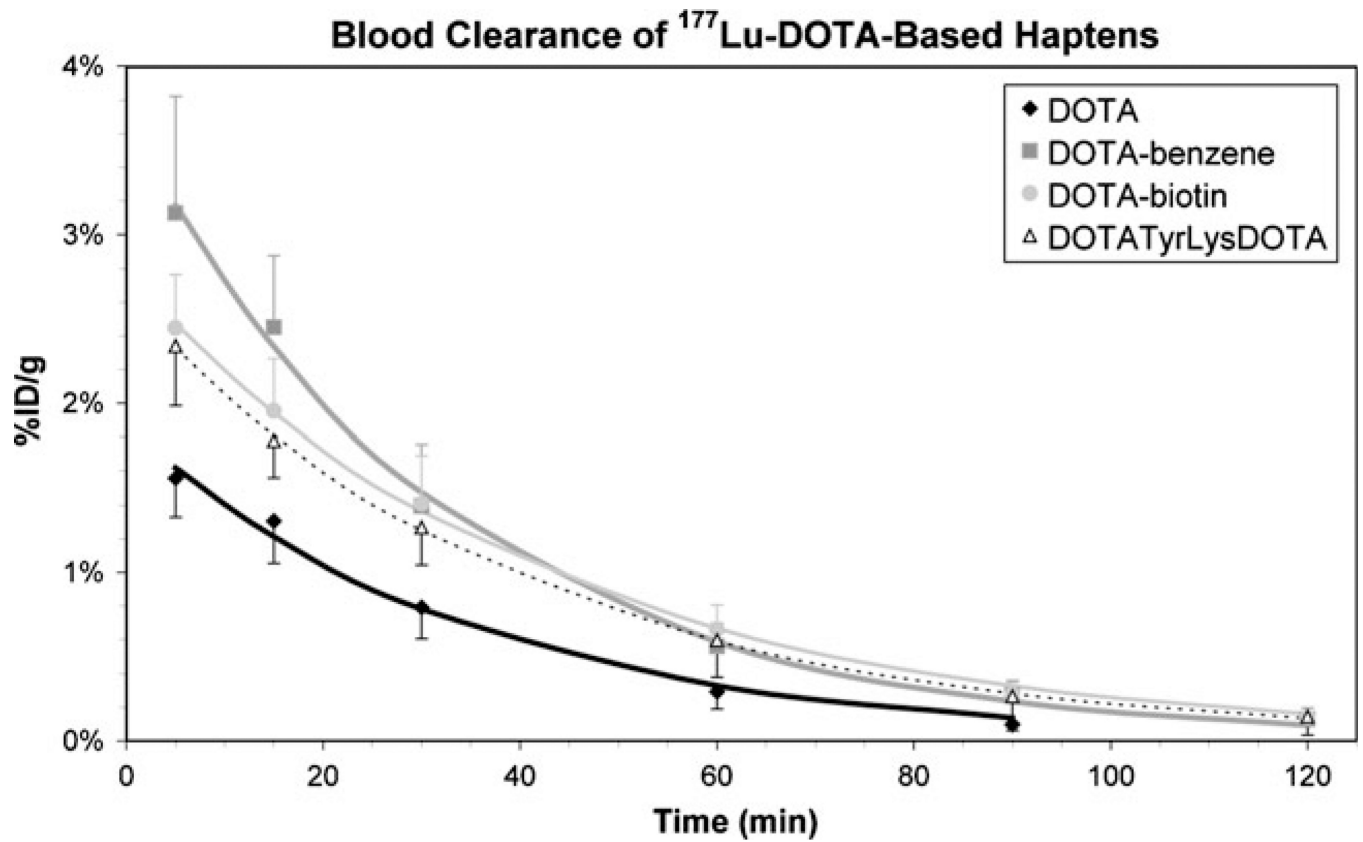


**Fig. 3.** *In vivo* clearance of intravenously injected haptens. Blood %ID/g (mean $\pm$ SD) time profile of haptens after intravenous injection of 50–150  $\mu\text{Ci}$  in CD1 mice ( $n = 3-4$ ). The lines represent fit exponential curves using least squares regression. By 2 h,  $^{177}\text{Lu}$ -DOTA blood activity was not distinguishable from background.

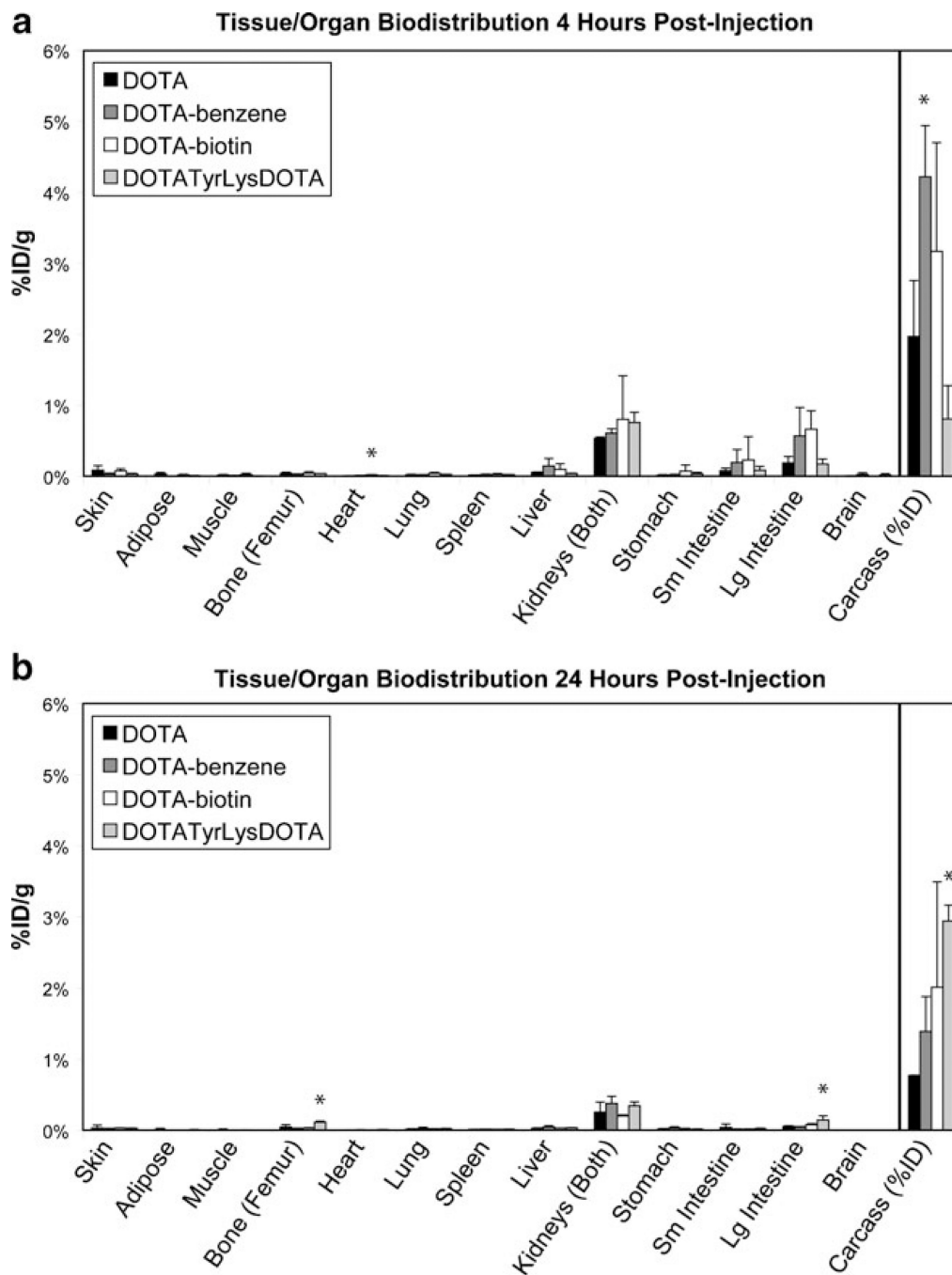


**Fig. 4.** *In vivo* tissue/organ biodistribution of haptens. Tissue/organ %ID/g (mean±SD) at 4 h postinjection (**a**) and 24 h postinjection (**b**) of 50–150  $\mu$ Ci hapten in CD1 mice ( $n=3-4$ ). Whole-body retention in carcass is presented as %ID. \* $P<0.05$  compared to  $^{177}\text{Lu}$ -DOTA.

**Table 1**

Estimation of whole-body retention in mice at 4 h postinjection for previously published small molecules

| Molecule   | %ID (whole body)  | Reference |
|--|-------------------|-----------|
| <sup>64</sup> Cu-DOTA-RGD  | >15               | [12]      |
| <sup>64</sup> Cu-DOTA-PEG-E(c(RGDyK)) <sub>2</sub>                       | >6.7              | [13]      |
| <sup>64</sup> Cu-DOTA-8-AOC-BBN  | >35               | [14]      |
| <sup>64</sup> Cu-CB-Te2A-8-AOC-BBN                                       | >13               | [14]      |
| <sup>67</sup> Ga-DOTA-PESIN  | >8.9              | [15]      |
| <sup>177</sup> Lu-DOTA-PESIN   | >8.8              | [15]      |
| <sup>99m</sup> Tc-depreotide   | >31               | [16]      |
| <sup>111</sup> In-DTPA-octreotide  | >13               | [16]      |
| Lys <sub>40</sub> (Ahx-DTPA- <sup>111</sup> In)NH <sub>2</sub> exendin-4 | >93               | [17]      |
| <sup>111</sup> In-IMP-241  | >1.4 <sup>a</sup> | [10]      |
| <sup>99m</sup> Tc-IMP-243  | >24 <sup>a</sup>  | [10]      |
| <sup>99m</sup> Tc-IMP-245  | >2.6 <sup>a</sup> | [10]      |
| <sup>125</sup> I-GP2 (galacto-cRGDyK)                                    | >7.6              | [18]      |
| <sup>68</sup> Ga-p-NO <sub>2</sub> -Bn-NOTA                              | >22               | [19]      |
| <sup>68</sup> Ga-p-NO <sub>2</sub> -Bn-Oxo                               | >98               | [19]      |
| <sup>68</sup> Ga-p-NO <sub>2</sub> -Bn-DOTA                              | >18               | [19]      |
| <sup>68</sup> Ga-p-NO <sub>2</sub> -Bn-PCTA                              | >36               | [19]      |

<sup>a</sup>Three hours p.i.



**Table 2**

## Blood clearance parameters

|                                  | <i>A</i>   | <i>t</i> <sub>1/2</sub> , alpha (min) | <i>t</i> <sub>1/2</sub> , beta (min) |
|----------------------------------|------------|---------------------------------------|--------------------------------------|
| <sup>177</sup> Lu-DOTA           | 0.95±0.01  | 0.17±0.06                             | 20.5±2.4                             |
| <sup>177</sup> Lu-DOTA-benzene   | 0.92±0.01* | 0.60±0.23*                            | 24.8±2.8                             |
| <sup>177</sup> Lu-DOTA-biotin    | 0.93±0.02  | 0.47±0.24                             | 28.3±2.8*                            |
| <sup>177</sup> Lu-DOTATyrLysDOTA | 0.93±0.01  | 0.21±0.03                             | 27.5±6.1                             |

\* *P*<0.05 compared to <sup>177</sup>Lu-DOTA

**Table 3**

Radiation dose estimates for DOTA-based chelates in selected organs

| Hapten        | Organ      | Organ self-dose (mGy/MBq) |                  |                   | Organ self-dose and cross-dose (mGy/MBq) |                  |                   |
|---------------|------------|---------------------------|------------------|-------------------|--|------------------|-------------------|
|               |            | <sup>90</sup> Y           | <sup>131</sup> I | <sup>177</sup> Lu | <sup>90</sup> Y                          | <sup>131</sup> I | <sup>177</sup> Lu |
| DOTA          | Liver      | 0.014                     | 0.011            | 0.0053            | 0.035                                    | 0.023            | 0.010             |
|               | Kidney     | 0.17                      | 0.11             | 0.067             | 0.19                                     | 0.12             | 0.071             |
| DOTA-benzene  | Red marrow | 0.00059                   | 0.00014          | 0.000096          | 0.0079                                   | 0.0070           | 0.0015            |
|               | Liver      | 0.026                     | 0.018            | 0.0091            | 0.052                                    | 0.035            | 0.016             |
| DOTA-biotin   | Kidney     | 0.24                      | 0.16             | 0.096             | 0.27                                     | 0.17             | 0.10              |
|               | Red marrow | 0.0011                    | 0.00027          | 0.00018           | 0.010                                    | 0.010            | 0.0021            |
| DOTATyLysDOTA | Liver      | 0.016                     | 0.011            | 0.0055            | 0.045                                    | 0.033            | 0.014             |
|               | Kidney     | 0.15                      | 0.088            | 0.054             | 0.18                                     | 0.11             | 0.063             |
| DOTATyLysDOTA | Red marrow | 0.0011                    | 0.00025          | 0.00017           | 0.011                                    | 0.013            | 0.0026            |
|               | Liver      | 0.018                     | 0.014            | 0.0068            | 0.052                                    | 0.043            | 0.018             |
| DOTATyLysDOTA | Kidney     | 0.23                      | 0.14             | 0.087             | 0.26                                     | 0.17             | 0.098             |
|               | Red marrow | 0.00097                   | 0.00023          | 0.00016           | 0.013                                    | 0.016            | 0.0032            |